MEASUEMENT AND COMPUTATION OF DYNAMIC RESPONSE OF ARCH DAMS INCLUDING INTERACTION EFFECTS*

Yusof Ghanaat[1], Robert L. Hall [2], Bruce B. Redpath[3]

ABSTRACT

A computation and experimental study of dam-water-foundation interaction conducted at Longyangxia Dam in China is described. In the primary tests, the dam and its retained water were excited by detonating large explosive charges in shallow water upstream from the dam. The dam and water responses to the explosives were recorded by accelerometers, pressure sensors, and three-component seismographs. In secondary tests, the average reflection coefficient of the reservoir boundaries was measured using a newly developed procedure based on the acoustic reverberation concept. The results obtained indicate that explosive detonations appear to be the best means for exciting the dam-water-foundation system, and that an acoustic reverberation technique offers a practical procedure for measuring the overall reflection coefficient for the entire reservoir. Dam displacement and acceleration responses and hydrodynamic pressures due to acceleration signals recorded at the base of the dam were computed using current analytical procedures. Generally, reasonable agreement between the measured and computed responses was obtained but the prediction could be improved if non-uniform input motion could be defined and used.

Key Words. Arch Dam; Dam-water-foundation interaction; Accelerations; Hydrodynamic pressures; Spectrogram; Reflection coefficient; Absorption coefficient; Acoustic reverberation; Explosives; Blast-generated motions; Field measurements

1. INTRODUCTION

This paper describes computation and field measurements of dam-water-foundation interaction effects that were performed on Longyangxia Dam -- a gravity arch dam located in Gonghe County, Qinghai Province, China. This study was done as the most recent phase of a continuing cooperative research program funded by the US National Science Foundation under the US-China Protocol on Earthquake Studies with additional support from the US Army Corps of Engineers, Waterways Experiment Station (WES). The collaborating organizations in this research project were QUEST Structures of Orinda, California, Institute of Water Conservancy and Hydroelectric Research (IWHR) of Beijing, China, and Waterways Experiment Station, Vicksburg, Mississippi.

The objectives of the research were: 1) to develop new testing procedures for exciting dynamic response of the entire dam-water-foundation system, 2) to explore a new and improved procedure for in-situ measurement of the average reflection-coefficient of the reservoir boundary, and 3) to obtain measured data that would enable better validation of the current analytical procedures for predicting earthquake response of arch dams.

The basic concept in the field measurements was to excite the dynamic response of the dam and its retained water by detonating explosive charges buried either in the foundation rock downstream from the

* *Journal of Seismology and Earthquake Engineering (JSEE): Summer 2000, Vol. 2, No. 3*
[1] Principal, QUEST Structures, 3 Altarinda Road, Suite 203, Orinda, CA 94563, USA
[2] Supervisory Research Structural Engineer, Structures Laboratory, Corps of Engineers Waterways Experiment Station, Vicksburg, Mississippi 39180, USA
[3] Principal, Redpath Geophysics, P.O. Box 540, Murphys, CA 95247, USA

dam or in shallow water upstream. The extremely narrow and steep gorge immediately downstream of the dam did not allow the use of explosives in bore holes as was done in a previous experiment at Dongjiang Dam in 1991 [1]. The explosive charges therefore were detonated in shallow water about 1.2 km upstream from the dam. In the primary program tests, large charges fired in water were intended to excite the dam-water interaction by blast-generated waves travelling through the foundation rock and water. In the secondary tests, the water interaction mechanism was excited by small explosive charges (blasting caps) suspended in the forebay. The major purpose of secondary tests was to determine the contribution to the dam-water interaction resulting from absorption of energy by the forebay bottom and sides, taking account of any sediment deposited at the bottom.

2. TEST STRUCTURE & INSTRUMENTATION

Longyangxia Dam is a 178 m-high concrete gravity arch dam completed in 1986. Longyangxia is the first dam in a cascade of seven dams planned for the upper reaches of Yellow River. As shown in Figure 1, the arch section of the dam is 396 m long at the crest level with a crest and base thickness of 15 m and 80 m, respectively. The dam also includes two 30-m high concrete gravity blocks at each end of the arch, beyond which auxiliary dams are provided on both banks. The total water front length of the dam structures is more than 1,223 meters. The dam includes an overflow spillway on the right abutment, two lower outlets on the right side near the base, and an intermediate outlet at mid-height near the left abutment.

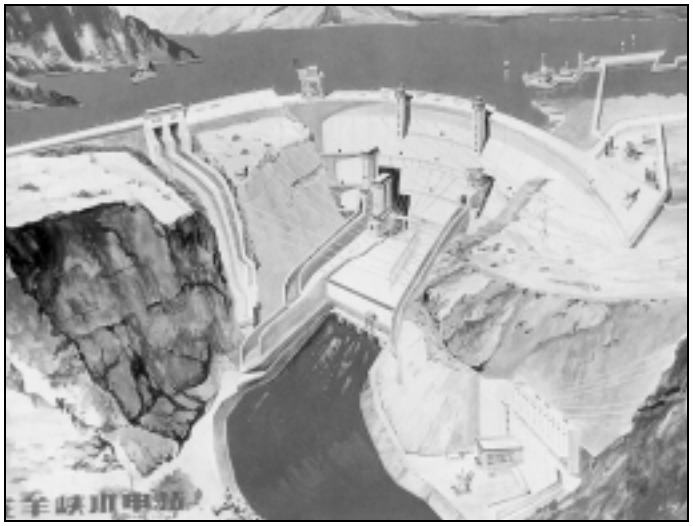

Fig. 1 Longyangxia Dam

The primary instrumentation used in recording the dynamic interaction were three sets of dynamic water pressure gages (hydrophones) installed on the face of the dam, within the forebay, and at the forebay entrance. A second instrumentation system consisting of accelerometers was employed to measure the dam response. The third recording system included a set of digital seismograph units positioned in galleries near the dam-foundation interface. Each of these instrumentation systems is described next.

2.1 Water pressures

Water pressures on the face of the dam were measured using two strings of hydrophones lowered from the dam crest and positioned approximately at the 1/4 span locations (Figure 2). Two additional strings of hydrophones were suspended within the forebay from a support cable stretched along the river channel at the mid-point of the dam at distances 25 m and 67 m from the dam face. These four hydrophone strings were connected to a PC-based data acquisition system located on the crest of the dam.

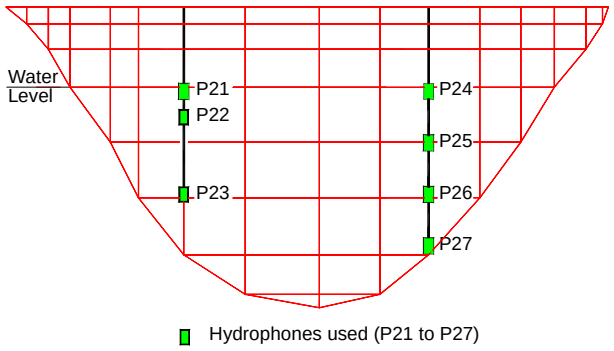

Fig. 2 Hydrophones suspended on face of dam

A third array of hydrophones, discussed later, was stretched across the forebay entrance to measure blast-generated waves travelling toward the dam. This horizontal array included 12 hydrophones spaced at 3m intervals with a Geometrics R-24 digital seismograph as the recording unit.

2.2 Dam accelerations

Instrumentation system used to measure the dam response consisted of 17 Wilcoxon accelerometers and a PC-based digital recording system. As shown in Figure 3, seven of these accelerometers (A1 to A7) were positioned along the crest of the dam and were oriented such that to sense the radial component of dam accelerations. The remaining 10 accelerometers were installed inside the galleries at four lower elevations, and were also oriented to measure the radial component of dam accelerations. The PC-based data acquisition system was placed in a room at the center of the dam crest.

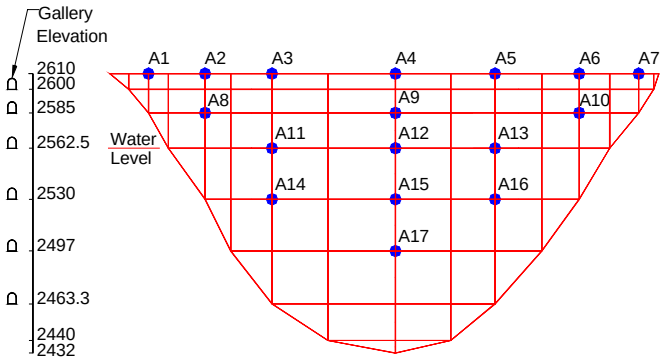

Fig. 3 Accelerometers mounted on dam crest and in galleries

2.3 Abutment motions

The abutment motions were recorded using 9 sets of three-component strong-motion seismograph units. These were positioned in galleries near the dam-foundation interface to provide some indication of the blast-generated waves applied to the dam and foundation rock. Each seismograph included a cassette tape recorder, a digital clock, and three accelerometers oriented in the radial, tangential, and vertical directions.

3. TEST PROGRAM

The experiment at Longyangxia Dam consisted of two types of explosion tests intended to excite either the entire dam-water-foundation system or the body of water adjacent to the dam (i.e. the forebay). In the primary tests, the dam-water and dam-foundation interactions were excited by detonating relatively large explosive charges in shallow water upstream from the dam. Initially, a 50-kg charge was detonated 2 km from the dam to calibrate the prediction of the resulting ground motion. The signals from this 50-kg calibration charge were much smaller than the ambient signals produced by turbine generators and other machinery. Therefore, it became clear that, if the use of excessively large amounts of explosives was to be avoided, only detonations at a closer distance would generate meaningful dam responses above the noise level. As a result the main blast tests of a single 100-kg, a single 300-kg, and double 300-kg charges were detonated at a distance of 1.2 km from the dam. Figure 4 is a plan view showing the dam crest and water level contour lines, location of shots, hydrophone array at the forebay entrance, and the blasting caps employed in the reverberation tests. The shot location was aligned approximately along the dam centerline so that the blast-generated waves propagating through the foundation rock would tend to excite the dam in the radial direction. The large explosive charges for the main tests were lowered from a boat and detonated on the lake bottom in approximately 30 m of water.

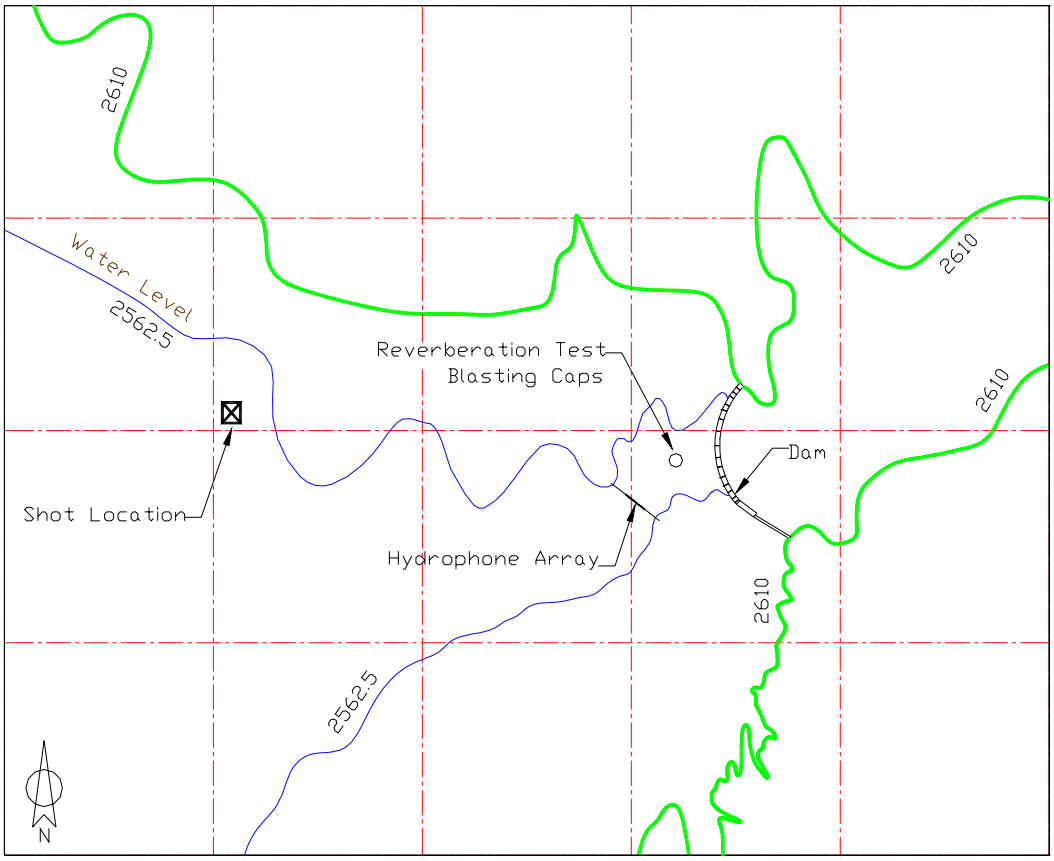

Fig. 4 Plan view of Longyangxia Dam and its retained water

In the secondary tests, the average reflection coefficient of the forebay at Longyangxia Dam was measured using a newly developed procedure based on the acoustic reverberation concept. Unlike our previous seismic reflection and seismic refraction techniques [1,2] that measured reflection coefficients at a spot or within a small region, acoustic reverberation employed in this experiment was an exploratory attempt to obtain an overall reflection coefficient for the entire forebay. In this novel technique the body of water near the dam is excited and brought to its steady state condition using an underwater energy source. The decaying pressure response produced by turning off the source is then measured by hydrophones to obtain the reverberation time, from which the reflection coefficient for any surface or combination of surfaces can be determined. The reverberation time refers to the amount of time required for the sound energy to decay 60 dB, or to one millionth of the original energy. In simple terms, this refers to the amount of time it takes for sound energy to bounce around a reservoir before being absorbed by the reservoir boundary materials. Closed spaces with highly reflective walls and boundaries have long reverberation times, and absorbent spaces have short reverberation times.

The acoustic reverberation tests used a vertical array of 10 blasting caps as the excitation source and an array of 12 hydrophones as detectors (Figure 5). Assembled at intervals of 3 m, the blasting caps were suspended in water and, using a sequential blasting machine, were detonated from bottom to top using delays of 100 ms and 50 ms. The resulting water pressures were recorded by the array of 12 hydrophones stretched across the forebay entrance and connected to the digital seismograph (also see Figure 4).

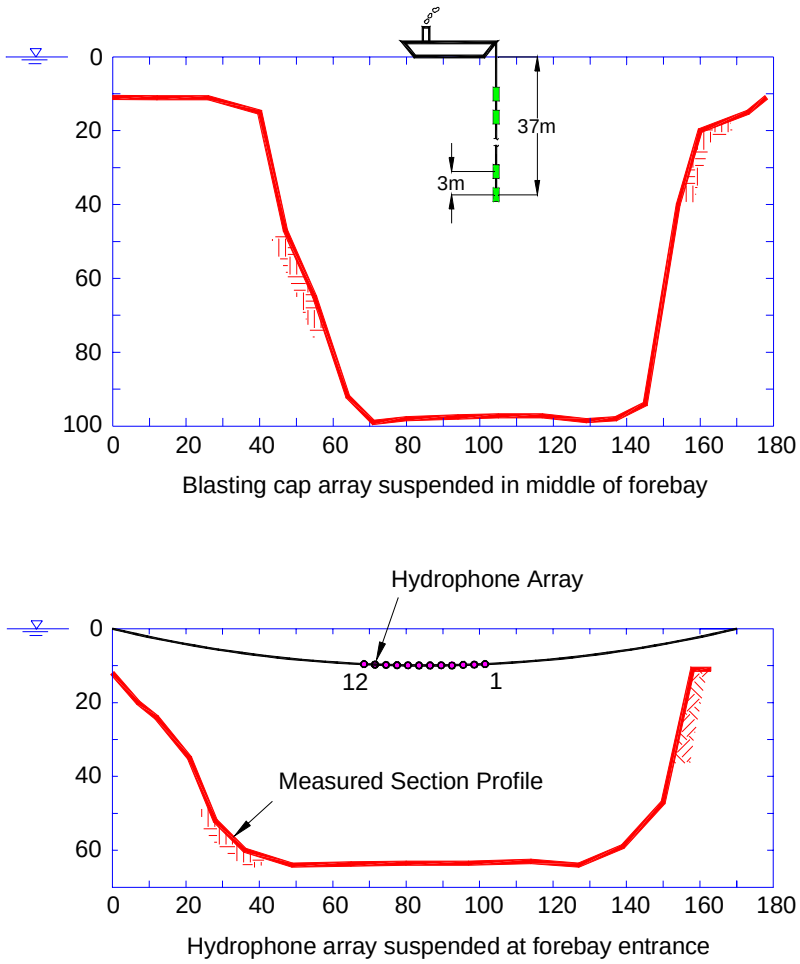

Fig. 5 Acoustic reverberation test setup

4. SUMMARY OF MEASURED DATA

This experiment has produced a complete set of measured data for the study of dam-water-foundation interaction effects. A total of 27 pressure responses, 17 acceleration responses, and 33 components of strong-motion seismograph records have been collected for each of the three main explosion tests. A comprehensive analysis and interpretation of all recorded signals is presented in a final report submitted to the U.S. National Science Foundation [3]. Only a few representative measured data are presented and discussed in this paper. Selected examples of the recorded signals for all three data acquisition systems are shown in Figures 6 and 8. As shown in Figure 6, the recording of dam accelerations and pressures on the face of the dam and within the forebay began approximately 10 seconds before the explosion and continued for a total duration of 30 seconds. Recording of water pressure at the forebay entrance (bottom graph in Fig. 6) was triggered automatically by the "zero-time" signal (top graph in Figure 6) and stopped after 8 seconds. Finally strong-motion seismograph recording was triggered manually about 1 second before the explosion and continued for a total duration of 10 seconds, but only the first four seconds of the seismograph signals are shown in Figure 8.

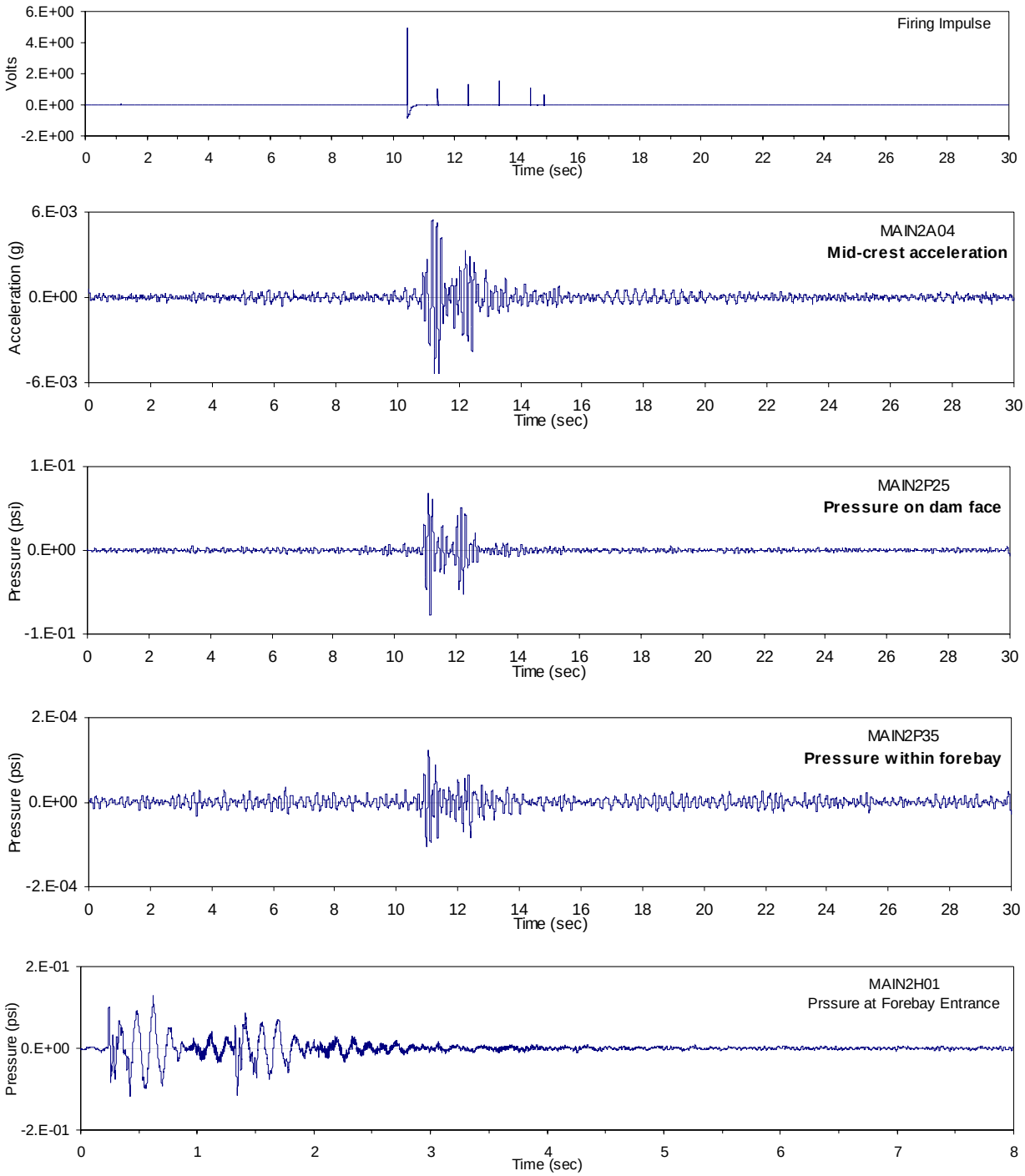

Fig. 6 Examples of recorded firing impulse, dam acceleration, and water pressures for single 300-kg charge

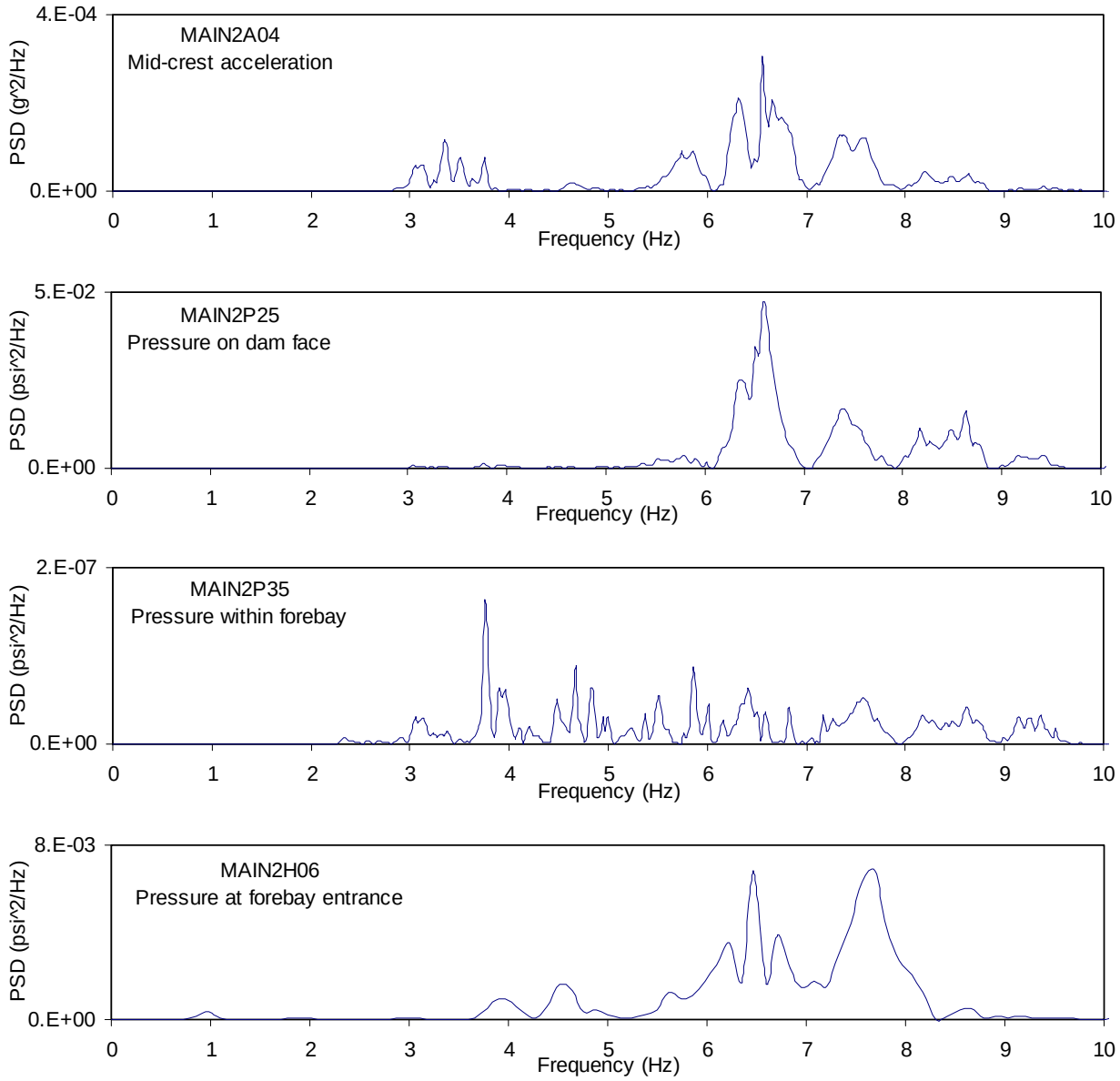

Fig. 7 PSD of recorded dam acceleration and water pressures

4.1 Recorded dam accelerations

In addition to dam accelerations and water pressures the "zero-time" or firing pulse was also recorded so that the exact detonation time and, therefore, the travel times of signals through foundation rock and water could be determined. This pulse was transmitted by wire over a distance of 1.2 km to the recording center. An example of the recorded acceleration at the center of the dam crest is shown in Figure 6 (2nd graph from the top). The velocity and displacement histories were computed by successive integration of the recorded acceleration in the frequency domain. The results indicate that maximum dam accelerations of about 0.002 g and 0.008 g were obtained for the 100 kg and 300 kg shots, respectively.

The acceleration signal in Figure 6 exhibits three distinct parts. The first part between zero and about 10.5 seconds is the dam response to ambient noise caused by turbine generators and other machinery. The second part with high-amplitude pulses starting at about 10.5 seconds and lasting about 3 seconds is the response of the dam to the blast-generated ground motion. The remaining signal beyond 14 seconds is again the dam response to the ambient noise, except that the dam response is higher from 17 to 21 seconds due to vibration of the outlet-gate towers.

4.2 Recorded water pressures

Figure 6 provides examples of water pressures recorded on the face of the dam, within the forebay, and at the forebay entrance. The recorded pressure signal at the forebay entrance suggests two explosions, even though only a single charge of 300 kg with no delay was used. Based on the time interval, water depth, and the weight of the charge, we believe that the second pulse starting at about 1 second (bottom graph of Figure 6) is the result of gas-bubble collapse. The high-frequency low-amplitude pulses at about 1 second indicate an arrival through the water, whereas the accompanying low-frequency high-amplitude pulses represent signals propagating through the foundation rock. The computed power spectral density (PSD) of the pressure signal at the forebay entrance (bottom graph of Figure 7) indicates that dominant frequencies of the blast-generated motion are in the range of 5 to 8 Hz. Accordingly, lower vibration modes of the dam below 10 Hz were excited satisfactorily, as indicated by PSD of the mid-crest acceleration (top graph of Figure 7).

The blast-induced pressure pulses are clearly visible in the recorded water pressure signals on the face of the dam and within the forebay (Figure 6). The PSD plots of these pressure records in Figure 7 indicate that, depending on their locations, the pressure signals contain a wide range of frequencies. The PSD plot of the dam-surface pressure generally resembles those of the dam acceleration recorded at the same location. The PSD plot of the pressure within the forebay, however, exhibits somewhat different frequency peaks. This observation indicates that, while the dam-surface pressures are proportional to the dam accelerations, the pressures within the forebay are partly influenced by the resonant characteristics of the impounded water, thus revealing clear evidence of water compressibility effects. For example the PSD of forebay pressure (second graph from bottom in Figure 7) shows a dominant peak at 3.7 Hz which closely relates to the theoretical resonant frequency of 100-m of water given by $f_r = C/(4H)$, where C is speed of sound in water and H is the depth of water.

4.3 Recorded abutment motions

The lack of access to the downstream region did not permit measurement of free-field ground motions at locations away from the dam where the effects of dam-foundation interaction had diminished. Instead, the abutment motions at nine locations along the dam-foundation interface were measured using three-component strong-motion seismographs. Figure 8 displays examples of time histories of the radial component of such recorded motions. The results show that the overall magnitudes, phasing, and frequency contents (not shown here) of abutment motions vary with elevation. The recorded motion at the top of an abutment is 1.7 to 3.9 times greater than the motion at the base of the dam. The pulse sequencing and phasing are somewhat different from location to location. The power spectrum of the upper abutment motions, not shown here, contains more peaks at a wider range of frequencies than the power spectrum of the base motion. Some of these peaks closely relate to vibration modes of the dam, while others appear to correspond to vibration of the abutment mass rock. These characteristics indicate that both the canyon topography and dam-foundation interaction effects are present in the recorded abutment motions. On this basis the abutment motions do not represent "free-field" motions. However, because the relative effects of topography cannot easily be separated from the dam-foundation interaction effects, the recording at the base of the dam, which is believed to be influenced very little by the topography and dam-foundation interaction, was employed as the input motion in the computer response predictions discussed later.

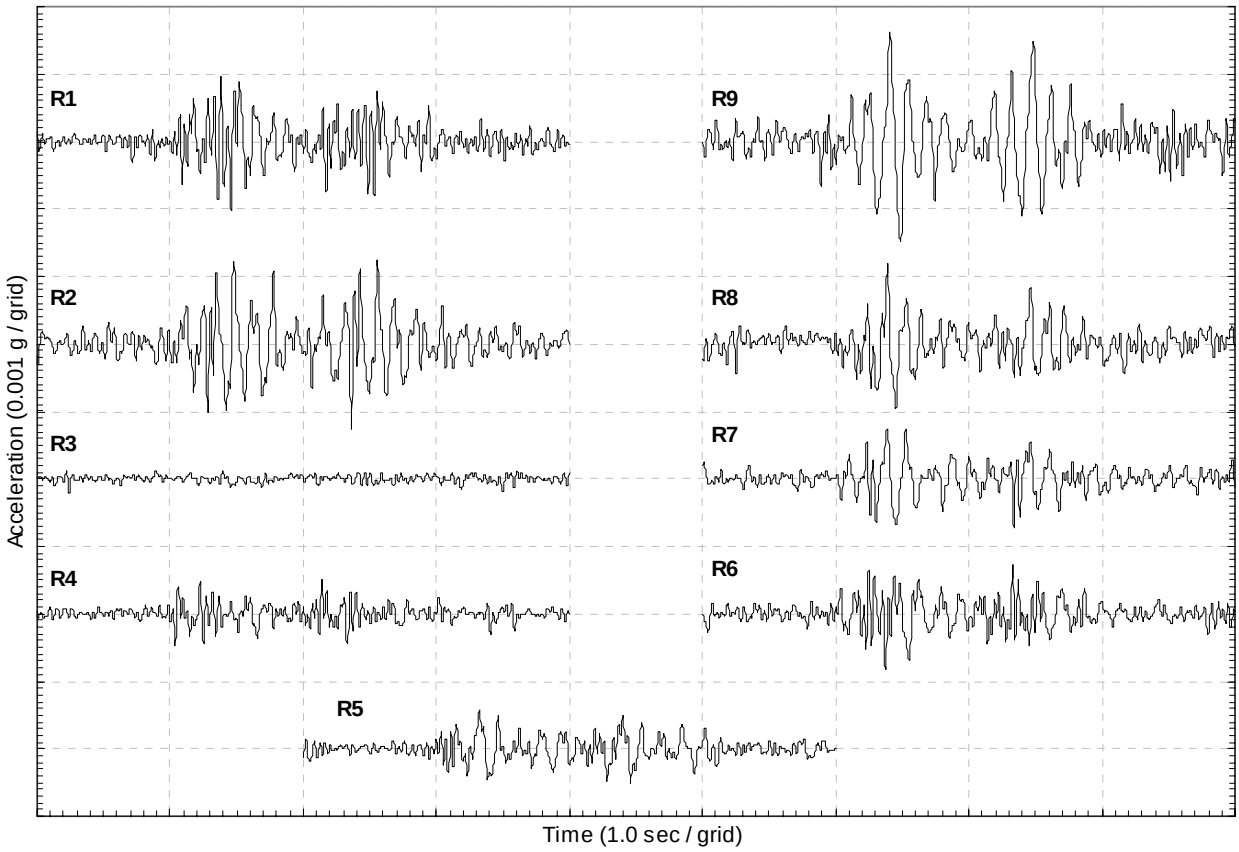

Fig. 8 Seismograph radial accelerations at dam-foundatin interface due to 300-kg charge

4.4 Dynamic characteristics of dam

Dynamic characteristics of the dam such as resonant frequencies, modal damping, and mode shapes can easily be identified from transfer functions, if input signal and dam responses at various locations are available. At Longyangxia Dam, only abutment motions at the dam-foundation interface locations could be measured. Consequently, these motions could not be characterized as the free-field input signals because they include contribution from the dam-foundation interaction. In the absence of the free-field input signal the power spectral density (PSD) function and cross-correlation spectrum between two response measurement points were used to obtain dynamic properties of the dam. A PSD peak at a given response point is identified as a resonant frequency of a mode of vibration if the phasing between this point and any other response point given by the cross-correlation spectrum is either zero or 180°. Following this procedure, the PSD functions and cross-correlation phase spectra were computed for all recorded dam acceleration signals. A peak frequency with zero- or 180°-phase angle, which consistently showed up in all records, was then identified as the best estimate of a resonant frequency.

Having identified the best estimate resonant frequencies, the mode shapes of Longyangxia Dam were determined by plotting displacement amplitudes of all recorded signals and orienting them according to their phase angles and thus creating three-dimensional deflected shapes. This procedure provided reasonable results as long as resonant frequencies of the dam were well separated and well defined. However, the identification of certain resonant frequencies and mode shapes became difficult and cumbersome when PSD functions showed closely spaced or overlapped peaks. This difficulty was resolved by decomposing the signal into its individual harmonics, each of which containing only a single frequency of interest. Such decomposition was achieved with the help of spectrograms. A spectrogram is a three-dimensional plot of PSD function with respect to frequency and time. A spectrogram of the recorded radial acceleration response at the mid-crest of the dam is shown in Figure 9. Spectrograms were also developed for the dam displacement responses. One difference between the acceleration and displacement spectrograms is that the high-frequency peaks dominate the acceleration spectrogram, whereas the displacement spectrogram tends to highlight the low-frequency peaks. The acceleration spectrograms therefore were employed for identification of the higher modes and displacement spectrograms for the lower modes. The acceleration spectrogram in Figure 9 clearly demonstrates the arrival of the blast signal at approximately 7.5 seconds with frequencies in the range of 5 to 8 Hz. The spectrogram also shows a persisting 3.1 Hz frequency between 8 and 21 seconds, indicative of the first mode of vibration.

With the amplitude and phase of the signal in frequency-time axis being known from the spectrogram, one could decompose the original signal into sub-signals of single frequencies and use them to identify modal parameters. This is accomplished by dissecting the spectrogram at the frequency of interest and plotting the resulting PSD functions in time axis as illustrated in Figure 10. The top graph in this figure shows the measured dam acceleration signal and the bottom graph the corresponding spectrogram for the 100-kg charge. Produced from the cross-section at 8 seconds, the second graph from the top exhibits frequency content of the measured signal at the time of 8 seconds. Whereas the second graph from the bottom obtained from the cross-section at 3.1 Hz, indicates spectral amplitude variations with time of a 3.1 Hz signal present in the recorded acceleration. Using such information the measured acceleration records were decomposed into dominant single-frequency records from which the dam response was animated and its mode of vibration determined.

Following the above procedure, 10 modes of vibration were identified, nine of which are displayed in Figure 11. Mode 1 at 3.17 Hz is the fundamental symmetric mode of the dam. Mode 2 with a frequency of 4.39 Hz represents the fundamental anti-symmetric mode of the dam. Mode 3 at 5.25 Hz is similar to the fundamental symmetric mode, except that it is accompanied by the second cantilever bending mode of the dam. Higher modes exhibit more complicated deflected shapes, but in general, they consist of higher order bending of the arch sections combined with the second and higher cantilever bending modes.

For each identified mode of vibration, an equivalent viscous damping ratio was determined by applying a single-degree-of-freedom curve fitting to a PSD peak representing that mode. The measured modal damping ratios varying in the range of 0.51% to 1.85% of critical are also shown in Figure 11.

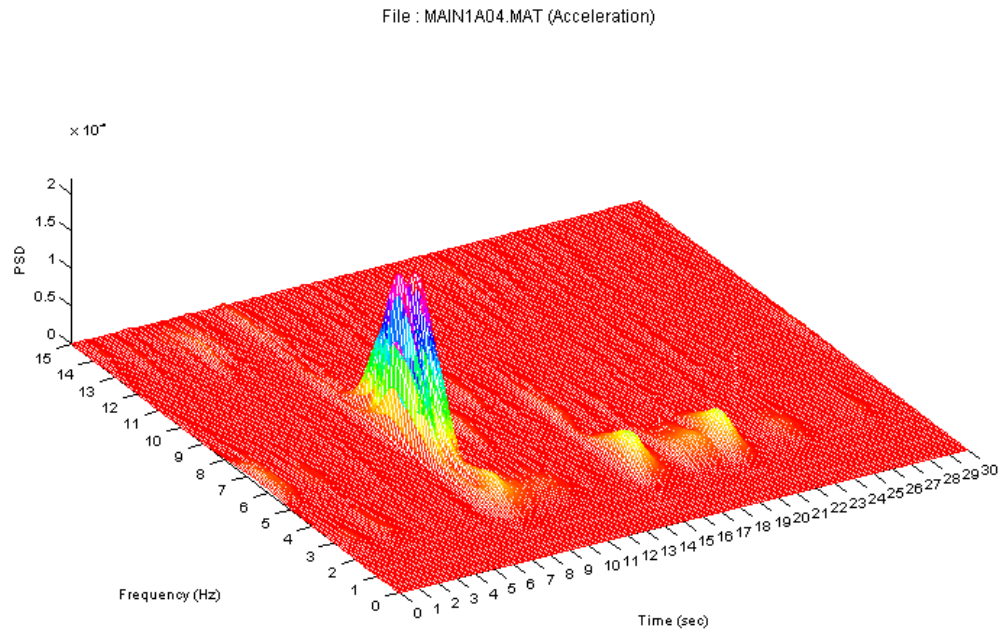

Fig. 9 3D spectrogram of recorded dam acceleration for 100-kg charge

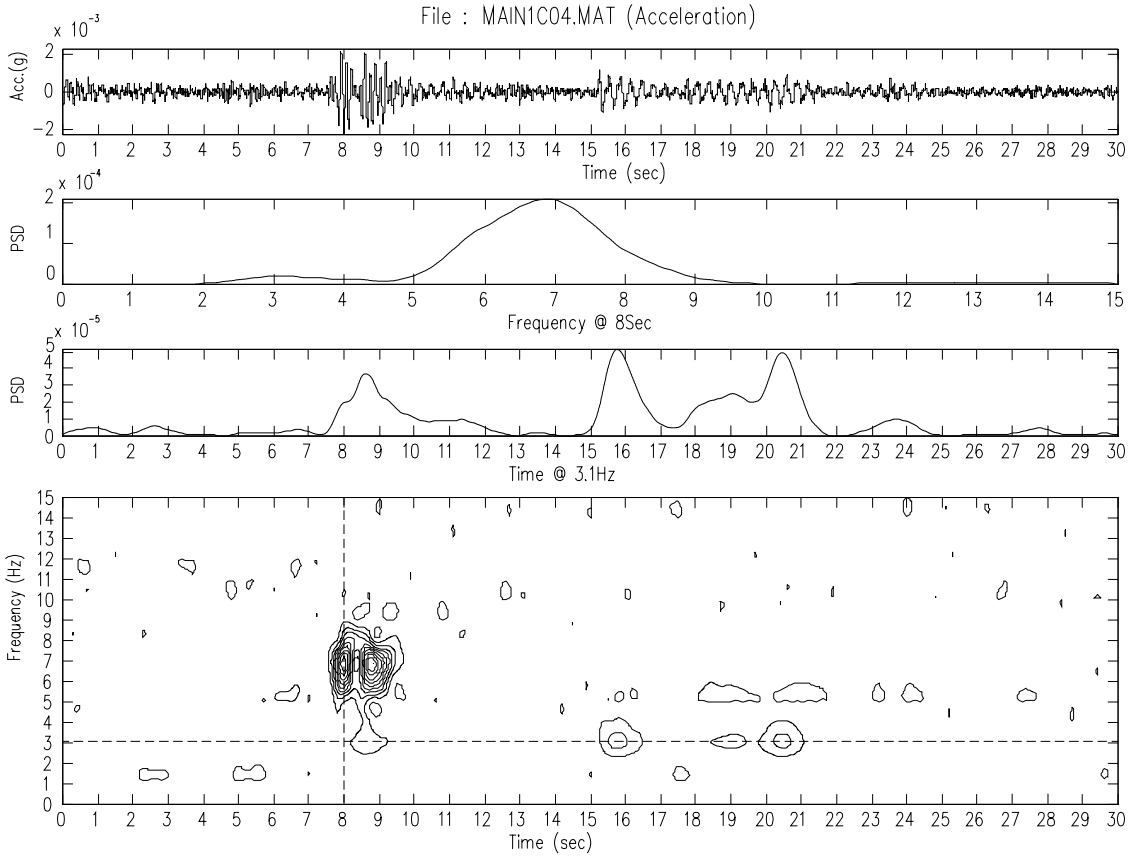

Fig. 10 2D Spectrogram of recorded dam acceleration for 100-kg charge

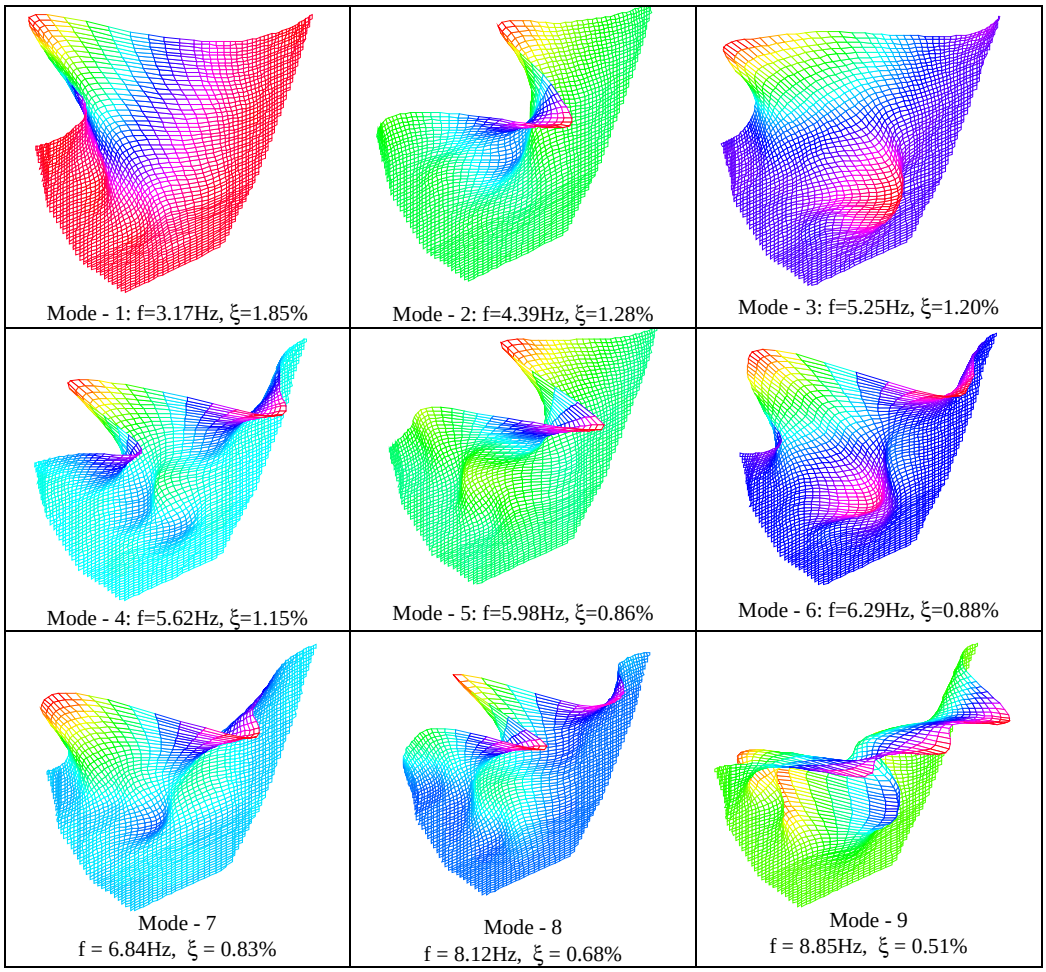

Figure 11. Measured mode shapes, frequencies, and modal damping ratios

4.4 Determination of wave reflection coefficient

The top graph in Figure 12 shows a pressure signal recorded by one of the 12 hydrophones stretched across the forebay entrance during the reverberation tests. This graph illustrates that the sequential detonation of 10 blasting caps did in fact produced a reasonably sustained signal, which then decayed at the conclusion of the detonation sequence. A PSD plot of the pressure signal in Figure 12 indicates that the sequential detonation has the effect of distributing the energy into numerous narrow-frequency bands separated by a frequency equal to inverse of the delay time. For example, the PSD plot for reverberation test with 100 ms delay shows well-separated peaks every 10 Hz. This frequency distribution of the energy provides a unique opportunity to establish variation of the reverberation time and thus reflection-coefficient with frequency by decomposing the recorded signals into separate frequency-band signals and studying them separately. Taking advantage of this property and using successive narrow band-pass filters, each recorded pressure signal was decomposed into numerous signals, each of which contained only one of the frequency peaks of the original signal. Transient signals obtained in this manner were processed and displayed as the acoustic energy to determine reverberation times at various frequency bands (Figure 13). For this purpose each decomposed signal was squared and averaged across all channels and then plotted in logarithmic scale. From the logarithmic graph, the reverberation time for each frequency band was determined, as the time required the acoustic energy to decay 60 dB.

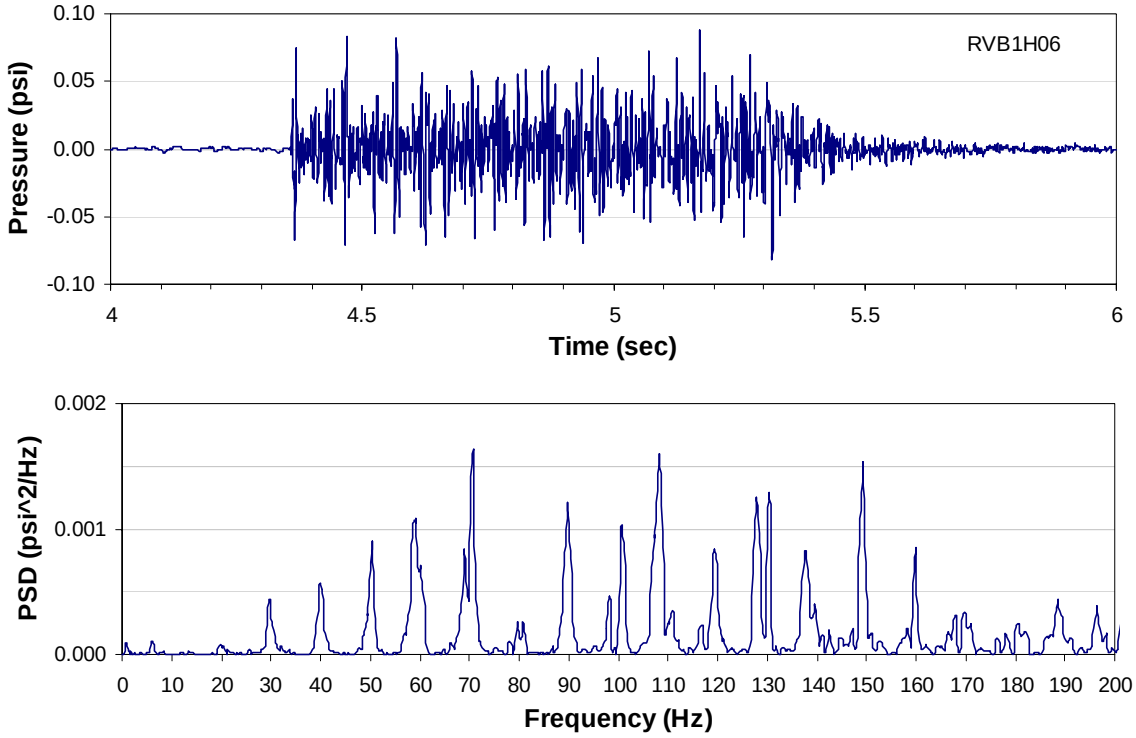

Fig. 12 Recorded pressure and computed PSD function at forebay entrance due to reverberation test shot with 100 ms delay

To establish the most likely trend between the reverberation time and the frequency, the estimated reverberation times at each frequency band were plotted as a function of frequency, as shown in Figure 14. The results for our exploratory reverberation tests show a linear relationship between the reverberation time and frequency.

Knowing the reverberation time and the volume of the forebay, the total absorption a for decay of sound energy in water is obtained using the well-known Sabine equation:

$$a = \frac{0.038V}{T} \qquad (1)$$

where V is volume of the forebay, and T is the reverberation time. Since absorption involves several surfaces with different acoustic properties, the total absorption a may be expressed as a summation of absorption for all interior surfaces of the forebay

$$a = \sum \alpha_i S_i \qquad (2)$$

where α_i is an energy absorption coefficient or a fraction of energy absorbed by surface S_i. Measuring reverberation time as discussed above and calculating the volume, the total absorption a for the entire forebay was first obtained using equation (1). Substituting the value of a in equation (2) the energy absorption coefficient of the forebay bottom was then estimated by assigning appropriate energy absorption coefficients to water and dam surfaces as well as the opening into the forebay. The energy absorption co-

efficients for the water surface and the opening into the forebay were set to zero and one, respectively. The energy absorption coefficient for the dam surface was estimated as 0.08 from the ratio of the acoustic impedances of concrete and water. The volume and surface areas were computed using a finite-element mesh of the forebay developed on the basis of the measured lake bottom profiles. Knowing the energy absorption coefficient, the energy reflection coefficient is obtained by considering that the energy absorption and reflection coefficients must add up to one. The amplitude reflection-coefficient is then obtained as the square root of the energy reflection-coefficient.

Figure 14 suggests a reverberation time of about 0.9 sec for frequencies below 20 Hz that are more representative of earthquakes. The use of 0.9 sec in the computational approach summarized above results in an energy absorption coefficient of approximately 0.32 for the sides and bottom of the forebay. This relates to an energy reflection-coefficient of o.68 which, in turn, would be the same as an amplitude reflection-coefficient of about $(0.68)^{1/2}$ or 0.82.

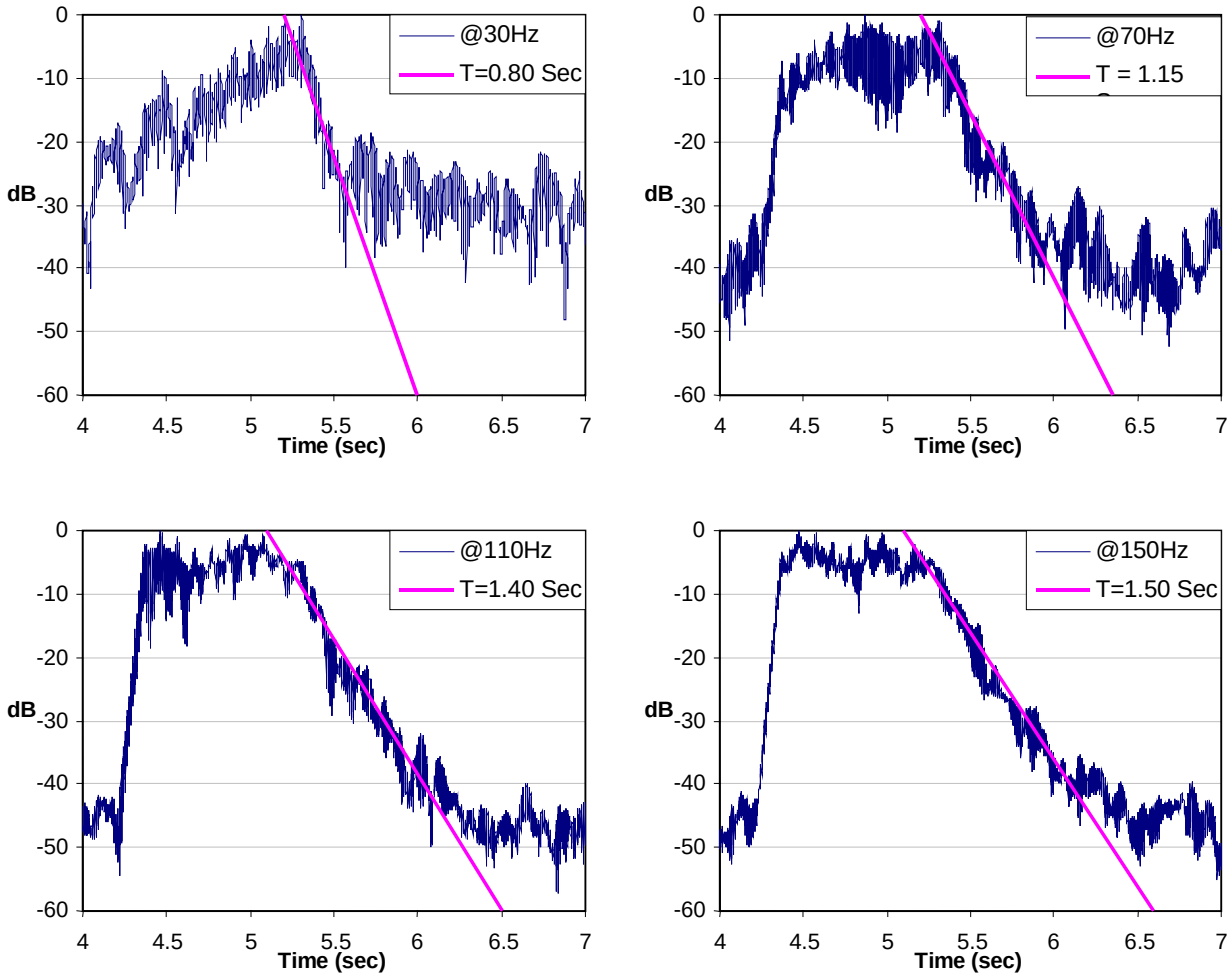

Fig. 13 Reverberation time at various frequency bands

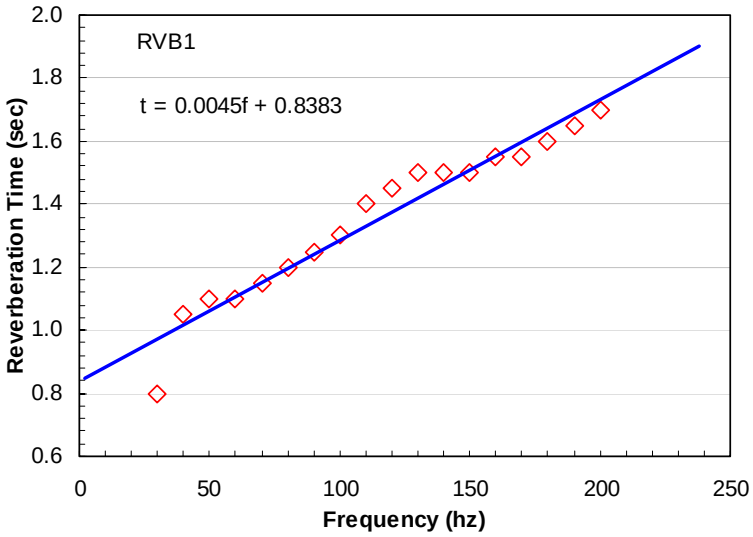

Figure 14. Variation of reverberation time with frequency

5. SUMMARY OF CORRELATION STUDIES

Another objective of this study was to obtain measured data for validation of the current analytical procedures. For this purpose Longyangxia Dam, its foundation rock, and the impounded water were modeled using the GDAP [4] and EACD-3D [5] programs, as shown in Figure 15. Both programs use the same finite-element models for the dam and foundation rock, except that GDAP employs incompressible water while EACD-3D considers water compressibility and reservoir boundary-absorption effects to represent the impounded water.

Models for the dam and foundation rock were developed in accordance with the standard finite-element procedures using shell and solid elements. The impounded water was modeled using either incompressible or compressible fluid mesh constructed to match the measured bottom topography of the forebay. A relatively close match between the measured and computed frequencies was obtained by increasing modulus of elasticity of the concrete and foundation rock by 40% (EACD-3D) and 63% (GDAP) beyond the static values. This increase of modulus is justified considering that the dynamic modulus is expected to be up to 50% higher than the static value.

Table 1 summarizes frequencies obtained from the numerical analyses and measurements. The measured frequencies are given for each main blast test. The values for all three tests are also summed and averaged as presented in last two columns of the table. The results indicate that both the GDAP and EACD-3D frequencies agree reasonably well with the measured values. Note that while the GDAP frequencies for the dam-water-foundation system were computed directly, the EACD-3D frequencies were obtained from the peak frequencies of the dam frequency-response functions. The GDAP mode shapes computed for the dam-water-foundation system (not shown here) also provided good agreements with the measured mode shapes discussed earlier.

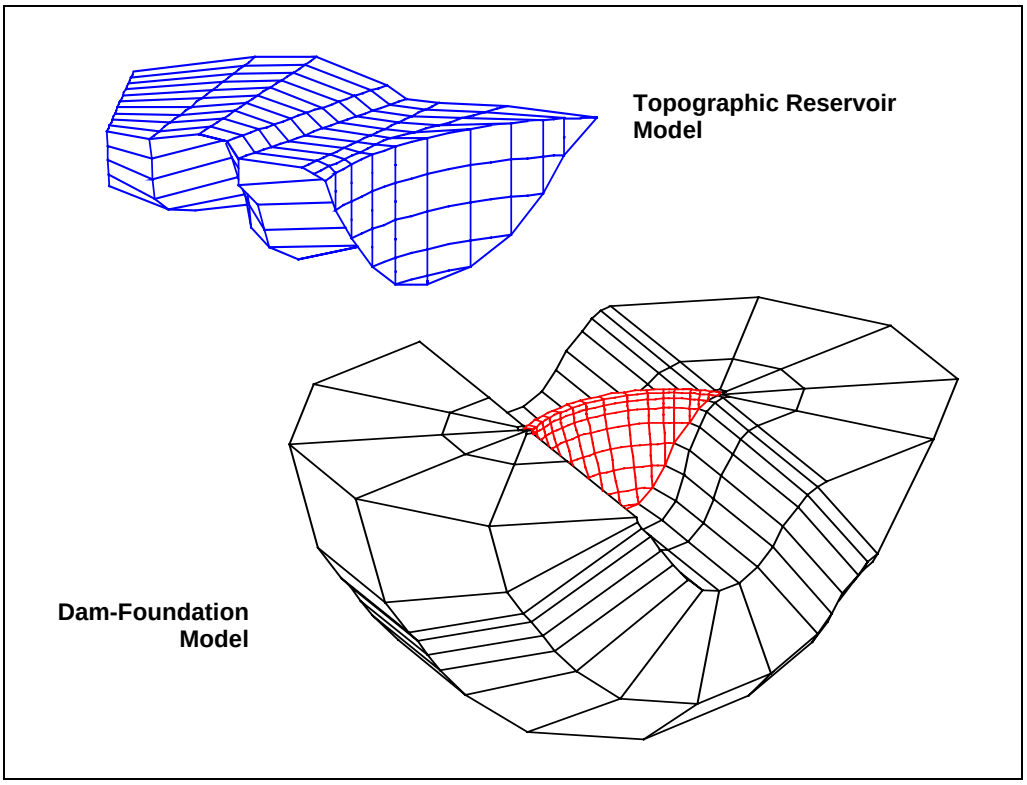

Fig. 15 Perspective view of dam-water-foundation model

Table 1 Summary of frequencies and damping ratios

Mode #	ANALYTICAL (Hw =130.5m)		MEASURED							
	GDAP	EACD-3D (α = 0.82)	100-kg Charge		Single 300-kg Charge		Double 300-kg Charge		Average	
	f (Hz)	f (Hz)	f (Hz)	ξ (%)	f (Hz)	ξ (%)	f (Hz)	ξ (%)	f (Hz)	ξ (%)
1	2.80	2.95	3.17	1.85	3.02	1.59	3.11	1.54	3.10	1.66
2	3.87	4.03	4.39	1.28	4.33	1.35	4.30	1.29	4.34	1.31
3	4.90	4.81	5.25	1.20			5.37	0.81	5.31	1.01
4	5.54	5.82	5.62	1.15	5.55	1.00	5.46	0.72	5.54	0.96
5	6.30	6.59	5.98	0.86	5.98	0.96	6.10	0.76	6.02	0.86
6	6.35	6.75	6.29	0.88	6.32	0.94	6.29	0.68	6.30	0.83
7	6.84	7.37	6.84	0.83	6.81	1.05	7.02	0.73	6.89	0.87
8	7.51	8.30	8.12	0.68	7.42	0.90	7.87	0.60	7.80	0.73
9	8.65	9.47	8.85	0.51	8.73	0.58	8.24	0.54	8.61	0.54
10	9.20	9.93	9.95	0.64	10.01	0.51	9.86	0.47	9.94	0.54

Dam displacement and acceleration responses and hydrodynamic pressures were computed by subjecting the dam-water-foundation model to input motion that consisted of the acceleration signals recorded at the base of the dam. Note that the water borne pressures did not produce any additional source of input on the face of the dam. This is because the water borne pressures almost completely vanished before reaching the dam, as indicated by the measured pressures at the forebay entrance. The radial, tangential, and vertical components of the base motion were applied uniformly in the stream, cross-stream, and vertical directions at the dam-foundation contact nodes. Various cases and conditions with and without water compressibility effects and fluid meshes based on a prismatic geometry or the measured reservoir topography were studied. Only results for the topographic fluid mesh with a measured reservoir-boundary reflection-coefficient of 0.82 and a measured average modal damping ratio of 2% are presented here.

Time histories of the measured and computed radial, vertical, and tangential displacements at the center of the crest are displayed in Figure 16. Overall, the GDAP model employing incompressible water provides a satisfactory match with the measured results, both in terms of amplitudes and waveforms. However, despite a more accurate formulation of the dam-water interaction effects, EACD-3D invariably produces larger displacements showing inadequate agreement with the measured values. Even such an agreement was achieved only after a large EACD-3D response at 6.6 Hz, not observed in the recorded signals, was removed from the results. Although such comparison is problem specific, it still could be concluded that more accurate analytical procedures are more sensitive to modeling assumptions and material properties and may not always produce better results than simpler numerical models. The differences between the measured and GDAP displacements are believed to be related to the use of uniform input motion, which ignores variation of the amplitudes and phasing along the dam-foundation interface. The unsatisfactory agreement between the measured and EACD-3D results is attributed to the use of uniform input motion but also to certain computed resonant frequencies that coincided with the peak of input spectra.

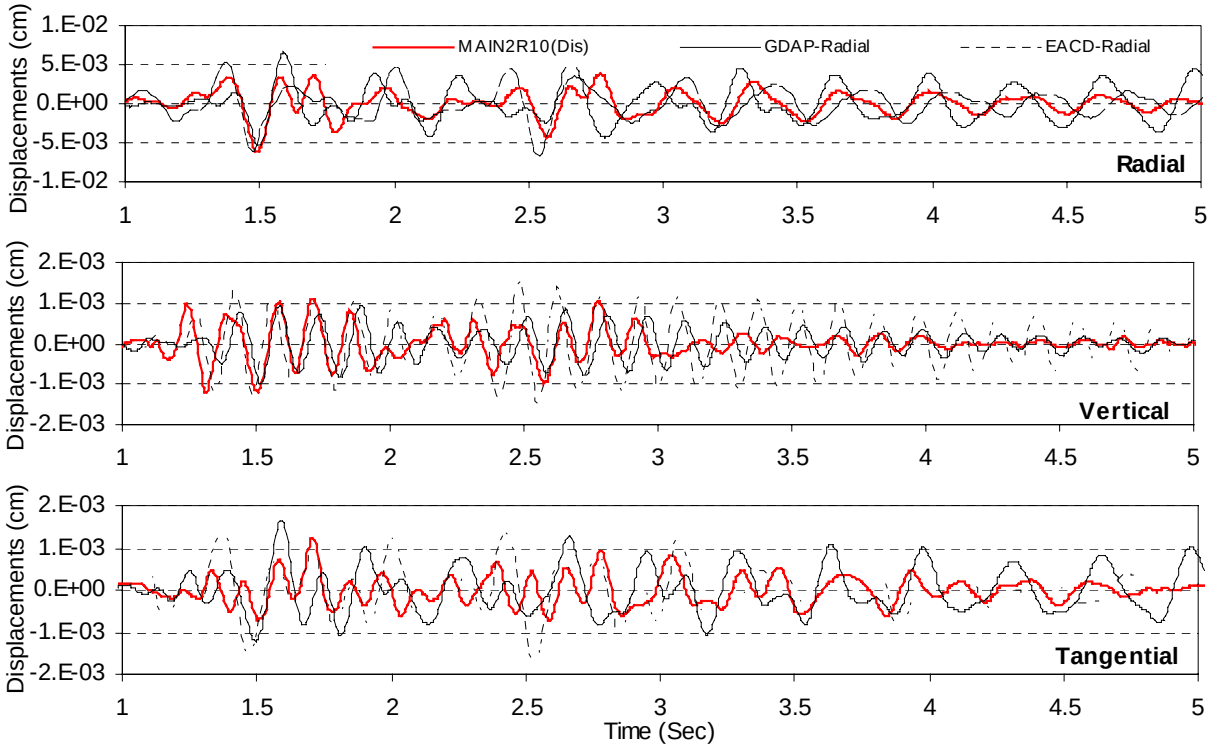

Figure 16. Comparison of measured and predicted crest displacements

Figure 17 compares the measured hydrodynamic pressures with the computed values for the topographic reservoir model due to the single 300-kg blast motion. The computed hydrodynamic pressures were obtained using the EACD-3D program. The results are presented for one location on the face of the dam and another within the forebay. The computed pressures agree reasonable well with the measured values only on the face of the dam. The computed pressures within the forebay are significantly greater than the measured values.

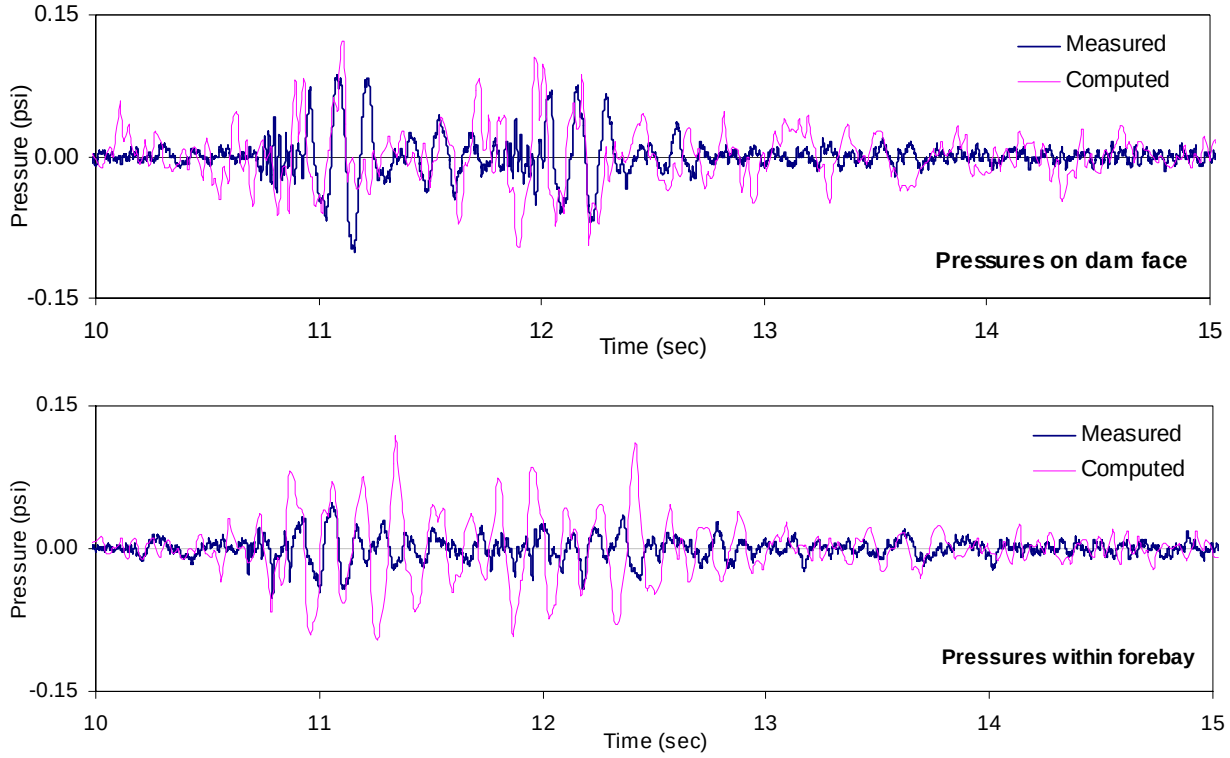

Figure 17. Measured and computed pressures on face of dam and within forebay

6. CONCLUSIONS

The program of computations and experimental measurements of the dam-water-interaction at Longyangxia Dam has accomplished the following:

- Demonstrated that the use of underwater explosions is an efficient method of exciting the complete dam-water-foundation system.

- Observed indications of water compressibility and the effects of interaction between the dam and foundation. The PSD's of the recorded pressures on the face of the dam contained dominant peaks at the resonant frequencies of the dam (dam-water interaction effects). The PSD's of the recorded pressures within the forebay clearly exhibited dominant peaks at frequencies that closely relate to theoretical resonant frequencies of the pressure waves propagating vertically and across the forebay. The recorded pressures therefore revealed clear evidence of water compressibility effects. The magnitudes, phasing, and frequency contents of abutment motions at the dam-foundation interface varied

with elevation and contained spectral peaks that closely related to the dam frequencies, thus indicating significant dam-foundation interaction effects.

- Developed a novel procedure for measuring the overall or average reflection coefficient of the reservoir boundaries in the immediate vicinity of the dam.

- Generated computer analyses that characterize the sensitivity of the dam response to various modeling assumptions. Overall, both the incompressible and compressible fluid models produced frequencies that differed less than 10% from the measured values. The compressible fluid model was generally less affected by the shape of the reservoir than the incompressible fluid model. Changes in reflection coefficient affected the prismatic and topographic reservoir models in the same way. The reflection coefficient mainly influenced the peak magnitudes of the frequency response functions with little or no modification of resonant frequencies. The results showed that the effects of reservoir geometry and wave reflection coefficient on the response of Longyangxia Dam to harmonic motions are significant. However, the effects of these parameters on the response of the dam to blast or earthquake ground motions will depend on the characteristics of such input motions and may somewhat differ from the response to harmonic motions. Overall, the GDAP-predicted results due to blast ground motion with prismatic reservoir were as good or better than the EACD-3D results with prismatic or topographic reservoir model.

REFERENCES

1. Ghanaat, Y., Chen, H.-Q., Redpath, B.B., and Clough, R.W. (1993). "Experimental Study of Dongjiang Dam for Dam-Water-Foundation Interaction," QUEST Report No. QS93-03 submitted to the US National Science Foundation.

2. Ghanaat, Y. and Redpath, B.B. (1995). "Measurements of reservoir-bottom reflection coefficient at seven concrete dam sites," QUEST Report No. QS95-01 issued to the US Army Corps of Engineers, Waterways Experiment Station and US Bureau of Reclamation.

3. Ghanaat, Y., Chen, H.-Q., Redpath, B.B., Hall, R.L., and Marjanishvili, S.M. (1999). "Measurement and Prediction of Dam-Water-Foundation Interaction at Longyangxia Dam," QUEST Report No. QS99-05 submitted to the US National Science Foundation.

4. Ghanaat, Y. (1993). "GDAP, Graphics-based Dam Analysis Program," US Army Corps of Engineers, Waterways Experiment Station, Vicksburg, Mississippi.

5. Fok, K.-L., Hall, J.F., and Chopra, A.K. (1986). "EACD-3D, A computer program for three-dimensional analysis of concrete dams," Eq. Eng. Research Center, University of Calif., Berkeley, Report No. UCB/EERC-86/09.